EPJ Web of Conferences **153**, 06029 (2017) DOI: 10.1051/epjconf/201715306029
ICRS-13 & RPSD-2016

A New Point Kernel Sampling Scheme and Monte Carlo Transport

Benoît Avez[1,⋆] and *Laurent* Bindel[1,⋆⋆]

[1] *Millennium, P.A. Courtabœuf, 16 avenue du Québec, 91 940 Villebon-sur-Yvette, France.*

Abstract. Starting from an existing point kernel intergrated over the bounding surface of a volume source [1], the present contribution proposes a new point kernel sampling scheme. This sampling scheme is shown to be more efficient than the standard one because the integration proceeds from line segment sources instead of point sources. A new kind of Monte Carlo transport process is proposed. It is called flux transport from a line source and is expected to be more efficient than the standard source transport.

1 Context

For some nuclear engineering purposes, the calculation speed can a parameter of importance. As examples of such applications, one can cite radiation protection, with virtual reality simulators where quick and yet accurate dose rate calculations are needed, or nuclear measurement softwares, that often rely on the calculation of transfer functions in order to process a given spectrum. For basically all softwares that need basically real-time results, the calculation time is crucial. As a consequence, researches aiming at finding new methodologies for point kernel calculation or Monte-Carlo transport are still topical to face the near-future of real-time embedded systems. In this paper, we present a new sampling scheme for the point kernel formula, discuss its advantages over the clasical one, and propose a new Monte-Carlo transport process.

2 New sampling procedure for the point kernel formula

The classical point kernel formula giving the collisionless scalar flux at a point detector of an isotropic, monoenergetic and volumetric source of spatial pdf $p(\mathbf{r})$ and total emission rate A is the well known formula:

$$\Phi(\mathbf{r}) = A \iiint \frac{p(\mathbf{r}')\, e^{-\int_\gamma \mu(s)ds}}{4\pi\|\mathbf{r}-\mathbf{r}'\|^2}\, d\mathbf{r}', \qquad (1)$$

where γ is the straight line path between the detector point $\mathbf{r}$ and the source point $\mathbf{r}'$ (hereafter referred to as the "straight line path", with $\mathbf{r}' = \mathbf{r} - s\,\mathbf{\Omega}$ and $\mathbf{\Omega} = \frac{\mathbf{r}-\mathbf{r}'}{\|\mathbf{r}-\mathbf{r}'\|}$, and where $\mu(s)$ is the total macroscopic photon cross-section at coordinate s of the straight line path γ. For a spatially homogeneous source distribution within the volume V_S, $p(\mathbf{r}) = \frac{1}{V_S}$ is constant. Taking $\mathbf{r}$ as the origin of coordinates, and expressing Eq. (1) in spherical coordinates leads to:

$$\Phi(\mathbf{r}) = \frac{A}{V_S} \iiint_{V_S} \frac{e^{-\int_\gamma \mu(s')ds'}}{4\pi s^2}\, s^2\, ds d\mathbf{\Omega}. \qquad (2)$$

For such a simple source distribution, it is interesting to see from Eq. (2) that, for a given solid angle, the integration over s is analytical. As a consequence, the partial contribution to the scalar flux of all possible source points of direction $\mathbf{\Omega}$ towards the detection point $\mathbf{r}$ reads[1]:

$$\begin{aligned}\varphi(\mathbf{r},\mathbf{\Omega}) &= \frac{A}{V_S} \int_\Gamma \frac{e^{-\int_\gamma \mu(s')ds'}}{4\pi s^2}\, s^2\, ds, \\ &= \frac{A}{4\pi\, V_S}\, e^{-\sum_{i\in[0;s_{in}]}\mu_i d_i} \times \frac{1-e^{-\mu_s(s_{out}-s_{in})}}{\mu_s}, \qquad (3)\end{aligned}$$

where Γ is the source segment that generates with respect to the detection point $\mathbf{r}$ all possible straight line paths γ of direction $\mathbf{\Omega}$. In the above equation Eq. (3), s_{in} and s_{out} stands for the abscissa of the entrance and exit points of the source volume along the line generated by $\mathbf{\Omega}$, μ_i stands for the total macroscopic photon cross-section of material i that is crossed along that line, and d_i the track length in material i (the sum over the indices i run over all materials that are crossed from the detector point up to the entrance of the source entrance, and index s is specific to the source volume). The latter Eq. (3) was used as an intermediate step to derive Eq. (5) of reference [1].

In a Monte-Carlo evaluation of the integral Eq. (2), this makes it possible to reduce the dimensionality of the problem. One can compute the associated marginal probability density $\tilde{p}(\mathbf{\Omega})$, integration of $p(\mathbf{r}) = \frac{1}{V_S}$ on the line of all possible sources points for a given solid angle $\mathbf{\Omega}$, which

⋆ e-mail: benoit.avez@millennium.fr
⋆⋆ e-mail: laurent.bindel@millennium.fr

[1] Here, we implicitely assume that the homogeneous source is distributed within a convex volume. A possible way to circumvent this assumption will be adressed further.

reads [2]:

$$\tilde{p}\,(\mathbf{\Omega}) = \int_{\Gamma} \frac{1}{V_S}\, s^2\, ds, = \frac{s_{out}^3 - s_{in}^3}{3\, V_S}. \quad (4)$$

The solution of Eq.(2) can be recast under the following lines:

$$\Phi(\mathbf{r}) = \iint \left[\frac{\varphi\,(\mathbf{r},\mathbf{\Omega})}{\tilde{p}\,(\mathbf{\Omega})}\right] \tilde{p}\,(\mathbf{\Omega})\, d\mathbf{\Omega}. \quad (5)$$

Sampling $\mathbf{\Omega}$ from the marginal pdf Eq. (4), which is exactly the probability density function obtained by uniformly sampling the source volume and considering only $\mathbf{\Omega}$ as a relevant variable, we are left with the following Monte-Carlo formula:

$$\Phi(\mathbf{r}) = \lim_{N\to\infty} \left[\frac{1}{N} \sum_{i=1}^{N} \frac{\varphi\,(\mathbf{r},\mathbf{\Omega_i})}{\tilde{p}\,(\mathbf{\Omega_i})}\right]; \quad (6)$$

with numerator and denominator obtained respectively from Eq. (3) and Eq. (4). This formula Eq. (6) is the main result of this paper. It is based on the so-called *use of expected values* (see, e.g., section 4.2 of ref. [2]) variance reduction technique.

3 Practical aspects of the new sampling procedure

3.1 Implementation of the formula

The implementation of the Monte-Carlo evaluation of the point-kernel formula using this sampling scheme is illustrated in Fig. 1 and follows Eqns. (3-4;6):

- Select a random point within the source volume - the choice of a given point is just a choice of a given solid angle;
- Compute the contribution to the scalar flux of this given solid angle Eq. (4) and its marginal probability density Eq. (3);
- Add the ratio of the two preceeding quantities to the current scalar flux evaluation, and iterate in order to reach the desired statistical precision.

One can notice that the implementation of this scheme is easy to achieve in existing point-kernel codes: only one additional surface has to be tracked (back) together with the use of Eq. (6).

3.2 Efficiency of the proposed point-kernel formula

In this section, the efficiency of the proposed point-kernel formula is illustrated through two test cases:

[2] Being a probability density, $\tilde{p}\,(\mathbf{\Omega})$ has the property $\iint \tilde{p}\,(\mathbf{\Omega})\, d\mathbf{\Omega} = 1$. One can also notice that Eq. (4) could be used (up to the $\frac{1}{V_S}$ factor) to estimate the volume of a given cell by isotropically sampling $\mathbf{\Omega}$ from a given point (possibly within the volume for more efficiency, in which case with $s_{in} = 0$).

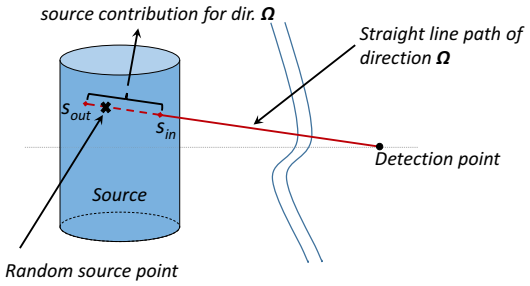

Figure 1. Illustration of the proposed point-kernel formula: for a given random source, contribution to the detection point comes from the full source segment between s_{in} and s_{out}.

- a 1st test case with a constant geometry with a source of varying density;
- a 2nd test case with a constant source material with several geometric extensions.

The efficiency of the method is evaluated by comparing the relative (statistical) error R of the proposed point-kernel formulation and the standard one for the same number of Monte-Carlo samples (100000).

3.2.1 1 m^3 cubic container filled with iron at several densities

The model, a cubic meter filled with iron at several densities is presented in Fig. 2. First, the proposed method

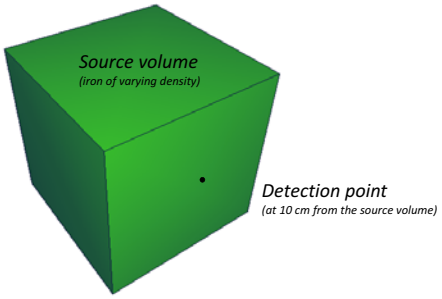

Figure 2. Test case #1: 1 m^3 cube of varying iron density. The detection point is located at 10 cm from the source volume.

is benchmarked for this test-case with iron at 8 $g.cm^{-3}$ against the standard point-kernel formula implemented in the same program, and is also benchmarked against MCNP6 [3] in similar conditions (i.e. uncollided photon flux of a F5 tally with simple physics treatment and energetic transport cut-off just below the considered energies). The results of the method comparison with respect

to standard point-kernel formulation (including the MCNP uncollided F5 evaluation) are presented in Table 1. A good

Table 1. Comparison of fluxes and relative errors of the improved point-kernel formulation with respect to the standard point-kernel method and MCNP. Number of Monte-Carlo samples is 10 millions.

E_γ	MCNP		Standard		Improved	
MeV	Φ	err.	Φ	err.	Φ	err.
0.1	1.57	1.0%	1.53	1.0%	1.54	0.04%
0.15	2.91	0.7%	2.87	0.7%	2.87	0.04%
0.2	3.82	0.6%	3.77	0.6%	3.78	0.04%
0.3	4.92	0.6%	4.87	0.6%	4.87	0.04%
0.4	5.66	0.5%	5.60	0.5%	5.60	0.04%
0.5	6.27	0.5%	6.21	0.5%	6.21	0.04%
0.6	6.81	0.5%	6.74	0.5%	6.74	0.04%
0.8	7.77	0.4%	7.70	0.4%	7.70	0.04%
1	8.64	0.4%	8.58	0.4%	8.57	0.04%
1.5	10.6	0.4%	10.5	0.4%	10.5	0.04%
2	12.0	0.3%	12.0	0.3%	11.9	0.04%

matching between the three methods is achieved in terms of fluxes (mean fluxes), and the small differences between MCNP and our implementations are likely due to different cross-sections and cross-section treatments. However, whereas standard point-kernel evaluations (MCNP and our implementation) have comparable relative errors, the relative error of the improved point-kernel formulation has, for this test case, an improvement of approximately a factor of ten.

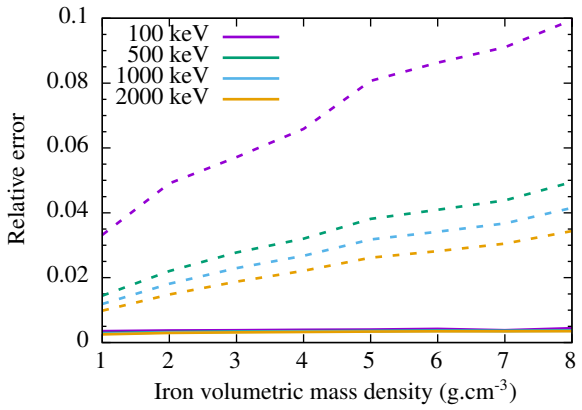

Figure 3. Evolution of the relative error with respect to the iron density - dashed: standard formula, solid: improved formula.

We now focus on test case #1, with iron densities ranging from 1 g.cm^{-3} to 8 g.cm^{-3}. Relative errors obtained at several energies for the standard point-kernel formulation and for the improved one are shown in Fig. 3. This figure shows that with the improved method :

i. the relative error is almost constant as a function of the iron density whereas it increases in the standard formulation case,

ii. the relative error is approximately the same for all considered energies, ranging from 100keV to 2MeV, whereas it is not the case for the standard formulation,

iii. the relative error is always smaller than the one obtained with the standard point-kernel formula, and

iv. best improvement of the proposed point-kernel formulation occurs at low energies, where the standard formulation is the less efficient.

3.2.2 $n \times n$ array of 1 m^3 cubic containers filled with concrete of density 1.5 g.cm^{-3}.

The model is presented in Fig. 4. The results of arrays

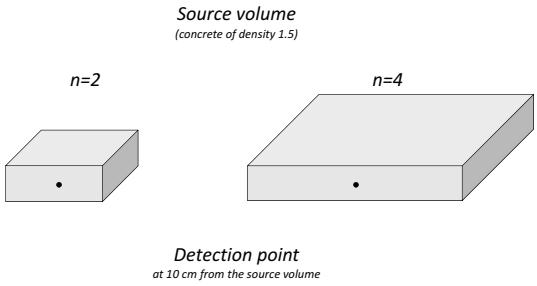

Figure 4. Test case #2: $n \times n$ array of 1 m^3 cubic containers filled with concrete of density 1.5 g.cm^{-3}. The detection point is located at 10 cm from the source volume.

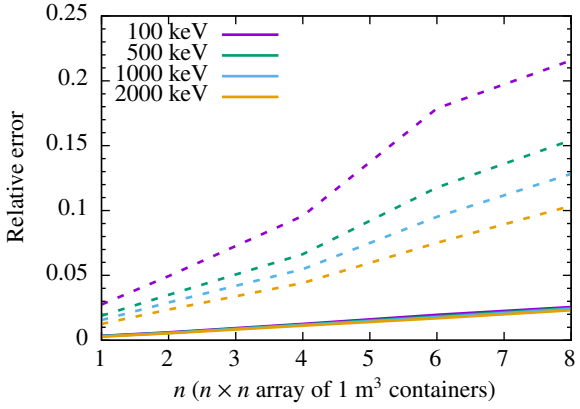

Figure 5. Evolution of the relative error with respect to the number of containers - dashed: standard formula, solid: improved formula.

of $n = 1$ to $n = 8$ are illustrated in Fig. 5. The latter shows a similar trends for the relative error as compared to the first test case. One difference, as compared to the preceding test-case, is the fact that the relative error is not

constant with respect to the size of the source, but slightly increases. This dispersion increase is due to the geometrical extension of the source.

4 Conclusion for the new sampling procedure

To summarize our main findings:

- Based on the use of expected values, we derived a new point-kernel formula by directly integrating all source contributions of a given solid angle to the scalar flux;
- This formulation can easily be implemented into an existing point-kernel based code: as compared to standard Monte-Carlo point-kernel evaluations, a *single* additional surface crossing has to be computed in the proposed formulation;
- The improvements, in terms of variance reduction, are particularly interesting for "optically thick" sources, i.e. for very absorbing source materials or for extended sources.

This technique has also the advantage not to depend on biaising parameters or on a specific mesh that are often also energy dependent, like in importance sampling. Finally, as already stated previously, the current derivation has been performed assuming a convex source volume. However, When the source volume is not convex, the same formula, without additional complexification, can still be applied. Indeed, in such cases, it is sufficient, for a drawn random source point, to compute the marginal probability density and the contribution to the scalar flux not on the full intersection between the generated straight line and the source volume (i.e. several disconnected segments), but only of the (connected) segment that contains the drawn point.

5 Towards a new Monte-Carlo transport process

The transport equation of an isotropic source reads:

$$[\mathbf{\Omega}.\nabla_{\mathbf{r}} + \mu_t(\mathbf{r},E)]\,\phi(\mathbf{r},E,\mathbf{\Omega}) = \iiint \mu_s(\mathbf{r},E'\to E,\mathbf{\Omega}'\to\mathbf{\Omega})\,\phi(\mathbf{r},E',\mathbf{\Omega}')\,dE'd\mathbf{\Omega}' + \frac{S(\mathbf{r},E)}{4\pi}, \tag{7}$$

where μ_t and μ_s are the total and scattering macroscopic cross-sections, S the source term, and whose left hand side inversion can be done (for instance, on a bounded domain with zero entering flux) using the the integral operator $\hat{T}_{\mathbf{r},E,\mathbf{\Omega}}[\,]$:

$$\hat{T}_{\mathbf{r},E,\mathbf{\Omega}}[\,] \equiv \int_\Gamma ds\, e^{-\int_\gamma \mu_t(s',E)\,ds'}\,[\,] \tag{8}$$

where the integral domain Γ of s is ranging from 0 to $|\mathbf{r}_b - \mathbf{r}|$, with $\mathbf{r}_b$ the zero incoming flux boundary in direction $-\mathbf{\Omega}$ with respect to $\mathbf{r}$ (and where s' is ranging from 0 to s). In order to simplify the notations, we now condense the notations. One defines the scattering operator $\hat{C}$:

$$\hat{C}_{\mathbf{r},E,\mathbf{\Omega}}[\,] \equiv \int dE' \iint d\mathbf{\Omega}'\,\mu_s(\mathbf{r},E'\to E,\mathbf{\Omega}'\to\mathbf{\Omega})\,[\,] \tag{9}$$

and, taking $P \equiv \mathbf{r},E,\mathbf{\Omega}$, the flux takes the following Neumann series formulation:

$$\begin{aligned}\phi(P) = &\quad \hat{T}_P\left[\frac{S}{4\pi}\right] \\ &+ \hat{T}_P\hat{C}_{P'\to P}\hat{T}_{P'}\left[\frac{S}{4\pi}\right] \\ &+ \hat{T}_P\hat{C}_{P'\to P}\hat{T}_{P'}\hat{C}_{P''\to P'}\hat{T}_{P''}\left[\frac{S}{4\pi}\right] \\ &+ \ ...\end{aligned} \tag{10}$$

Since $\hat{T}_P\left[\frac{S}{4\pi}\right]$ is the (uncollided) flux, the preceeding form Eq. (10) suggests that (i) the uncollided (directed) flux $\varphi(P) = \hat{T}_P\left[\frac{S}{4\pi}\right]$ can be taken, from Eq. (3), as the 0^{th} order quantity, and (ii) higher orders are built of successive applications of $\hat{T}_P\hat{C}_{P'\to P}$ applied to $\varphi(P)$. This makes it possible to compute the total scalar flux from Eq. (10):

$$\begin{aligned}\Phi(\mathbf{r},E) = \iint d\mathbf{\Omega} \quad &\{\varphi(P) \\ &+ \hat{T}_P\hat{C}_{P'\to P}\varphi(P') \\ &+ \hat{T}_P\hat{C}_{P'\to P}\hat{T}_{P'}\hat{C}_{P''\to P'}\varphi(P'') \\ &+ \ ...\}\end{aligned} \tag{11}$$

This formulation can serve as the basis of a new Monte-Carlo sampling scheme in which a flux is transported instead of a particle, and in which a contribution to the tally is done at each collision, in the spirit of next-event estimators (see e.g. Eq. (5.80) of [4]). The latter can take advantage of the source line flux evaluation Eq. (3) for the evaluation of the (directed) uncollided flux φ. Efforts are currently being done in that direction.

References

[1] L. Bindel, A. Gamess, E. Lejeune, J. Nucl. Sci. Technol. **37** suppl. 1, p. 512-514 (2000)
[2] M. H. Kalos and P. A. Whitlock, *Monte Carlo methods. Second edition* (WILEY-VCH, 2008)
[3] T. Goorley, et al., *Initial MCNP6 Release Overview*, Nuclear Technology **180**, p 298-315 (2012)
[4] M. H. Kalos, F. R. Nakache and J. Celnik, *Computing Methods in Reactor Physics*, Chapter 5 (GORDON AND BREACH, 1968)